

Harmonised corrections:

Reviewer 1

1. The presentation of data analyses have been improved. See line 173 – 178.
2. Line 16: Magnetic dip of Birnin-Kebbi have been included.
3. Lines 53 – 56: The authors have included some references discussing the ionosphere during quiet and disturbed conditions.
4. Lines 104 – 114 shows more references have been sited.
5. In line 151, a reference have been cited for equation 4
6. Line 173: We specified that we are using hourly OBS-TEC and hourly IRI-2016 model.
7. Line 189: The whole paragraph have been rephrased, the line talking about day-to-day variation with error bar (line: 193) have also been written clearly.
8. In Lines 198 – 204, the definition of all time and values have been written in a clearer manner. Also, in line 200: The time of occurrence of maximum TEC have been corrected.
9. The daily profile of IRI-2016 in Figures 1 – 4 obtained from IRI website (URSI option) is correct. It is not shifted in time.
10. In line 289 – 295, the paragraph have been written clearly. The time difference for post-midnight and pre-midnight hours have been clearly stated.
11. Line 300 – 304 have been written clearly with Table III to summarize.
12. Figure 10 have been potted on a single frame.
13. Line 312 – 319: Explains the direct impact of solar phenomena in the ionosphere with references.
14. The whole paragraph in line 312 – 319 have been corrected.
16. At this point, the conclusion now captures our corrected results.

Reviewer 2

1. Methodology: Line 173 – 178 have been revised. Statement about error bars have been deleted.
2. Line 193 explains OBS-TEC error bars signifies standard deviation from mean values.
3. Line 200: Maximum time of occurrence have been changed to 12 – 14 LT.
4. Line 307: “1 TECU variation represents an error of 0.16m in position” replaces “1 TECU = 0.16m”
5. Figure 10 now shows data points connected with line
6. Lines 312 – 313 now reflect the text “Figure 10 shows the comparison of the monthly OBS-TEC and sunspot number, Rz from 2011 – 2014, showing an increase of TEC with solar cycle”.
7. The conclusion now includes the scientific contribution of this investigation.
8. Some text in the discussion section have been deleted.

Reviewer 2.2:

1. Line 117 – 118 in the introduction shows our result is similar to result of authors in line 113 – 114. This is further discussed in the result and discussion section (line 252 – 257).
2. Lines 193 – 194: It is clarified that error bar represent the standard deviation of OBS-TEC from mean values.

3. Lines 214 – 215 have stated that maximum OBS-TEC of most of the months shifted to slightly post-noon. Further lines added reference to the sentence regarding peak shifting in Polar Regions.
4. Lines 225 – 235: The time of suitable IRI predictions have been corrected appropriately. When the IRI curve fit within the error bar of OBS-TEC, the model is said to be suitable.
5. Figures 5 – 8 have included horizontal line.
6. Line 231 defines pre-midnight hour.
7. Line 148: shows “and” have been inserted between satellite bias and receiver interchange bias.
8. Line 176: duplicate word “using” have been deleted.
9. Line 209: Rayleigh-Taylor Instability replaces wrong spelling.
10. Misplaced Y label in Figure 2b have been deleted.
11. Line 271 – 272 have been changed to “minimum and maximum seasonal VTEC values during June solstice and December solstice respectively”

DIURNAL, SEASONAL AND SOLAR CYCLE VARIATION OF TOTAL ELECTRON CONTENT AND COMPARISON WITH IRI-2016 MODEL AT BIRNIN-KEBBI

^{1,*}Aghogho Ogwala, ¹Emmanuel Olufemi Somoye, ³Olugbenga Ogunmodimu, ¹Rasaq
Adewemimo Adeniji-Adele, ¹Eugene Oghenakpobor Onori, ²Oluwole Oyedokun

^{1,*} Department of Physics, Lagos State University, Lagos, Nigeria.

² Department of Physics, University of Lagos, Nigeria.

³ Department of Electrical Engineering, Manchester Metropolitan University, United Kingdom.

ABSTRACT

Total Electron Content (TEC) is an important ionospheric parameter used to monitor possible space weather impacts on satellite to ground communication and satellite navigation system. TEC is modified in the ionosphere by changing solar Extreme Ultra-Violet (EUV) radiation, geomagnetic storms, and the atmospheric waves that propagate up from the lower atmosphere. Therefore, TEC depends on local time, latitude, longitude, season, geomagnetic conditions, solar cycle activity, and condition of the troposphere. A dual frequency GPS receiver located at an equatorial station, Birnin-Kebbi in Northern Nigeria (geographic location: 12.64° N; 4.22° E; 2.68° N dip), has been used to investigate variation of TEC during the period of 2011 to 2014. We investigate the diurnal, seasonal and solar cycle dependence of observed (OBS) TEC and comparison with latest version of International Reference Ionosphere (IRI-2016) model. On a general note, diurnal variation reveals discrepancies between OBS-TEC and IRI-2016 model for all hours of the day except during the post-midnight hours. Slight post-noon peaks in the daytime maximum and post-sunset decrease and enhancement are observed in the diurnal variation of OBS-TEC of some months. On a seasonal scale, we observed that OBS-TEC values were higher in the

equinoxes than the solstices only in 2012. Where as in 2011, September equinox and December solstice recorded higher magnitude followed by March equinox and lowest in June solstice. In 2013, December solstice magnitude was highest, followed by the equinoxes and lowest in June solstice. In 2014, March equinox and December solstice magnitude were higher than September equinox and June solstice magnitude. June solstice consistently recorded the lowest values for all the years. OBS-TEC is found to increase from 2011 to 2014, thus revealing solar cycle dependence.

KEYWORDS: TEC; diurnal; seasonal; variation; solar cycle 24; IRI-2016.

CORRESPONDING AUTHOR PHONE: +234 8055650264

CORRESPONDING AUTHOR E-MAIL: ogwala02@gmail.com

1 INTRODUCTION

The ionosphere causes a variation in the intensity of radio signals – fading – as a result of irregularities (inhomogeneity in electron density) (Somoye, 2010; Ogwala et al. 2018, Ogunmodimu et al. 2018). Akala et al., (2011) reported that the variable nature of the equatorial/ low latitude ionosphere threatens communication and navigation/ satellite systems. The equatorial/ low latitude ionosphere exhibits many unique features such as the seasonal anomaly, semi-annual anomaly, equinoctial anomaly, noon bite-out, spread-F, equatorial electrojet (EEJ), equatorial plasma bubbles (EPB) (Stankov, 2009; Maruyama et al., 2004; Jee et al., 2004; Codrescu et al., 1999).

For many decades, scientists have been studying these ionospheric features and the role they play in trans-ionospheric electromagnetic radio wave propagation. These studies are carried out using different techniques and instruments. One of the instruments used is the GPS receiver, which provide direct measurements from satellites. Their sounding capacity extends to the topside of the ionosphere, but is affected by time and space constraints (Ciraolo and Spalla, 2002). Recently, GPS receiver is the most efficient method used to eliminate the effect of the ionosphere on radio signals. This method combine signals in different L band frequencies, L1 (1575 MHz) and L2 (1228 MHz).

Almost all space geodetic techniques transmit signals in at least two different frequencies for better accuracy (Alizadeh et al., 2013). These are combined linearly and can greatly eliminate the effect of the ionosphere on radio signals. The ionospheric effect on radio signal is proportional to total electron content (TEC), which is defined as the number of electrons per square meter from satellite in space to receiver on ground is shown in Eq. (1).

$$TEC = \int n_e(s)ds \quad (1)$$

It is measured in multiples of TEC units ($1 \text{ TECU} = 10^{16} \text{ el/m}^2$). Due to the dispersive nature of the ionosphere, there is a time delay between the two frequencies of a GNSS signal as it propagates through the ionosphere as shown in Eq. (2) as $\Delta t = t_2 - t_1$. Thus,

$$\Delta t = \left(\frac{40.3}{c} \right) \times \frac{TEC}{\left[\left(\frac{1}{f_2^2} \right) - \left(\frac{1}{f_1^2} \right) \right]} \quad (2)$$

Where c is speed of light and f is frequency. Hence, Δt measured between the L1 and L2 frequencies is used to evaluate TEC along the ray path.

When Global Navigation Satellite System (GNSS) signals propagate through the ionosphere, the carrier experiences phase advance and the code experiences a group delay due to the electron density along the line of sight (LOS) from the satellite to the receiver (Bagiya et al., 2009; Tariku, 2015). Thus, the carrier phase pseudo ranges are measured too short, and the code pseudo ranges are measured too long compared to the geometric range between the satellite and the receiver. This results in a range error of the positioning accuracy provided by a GPS receiver. The range error due to TEC in the ionosphere varies from hundreds of meters at mid-day, during high solar activity when the satellite is near the horizon of the observer, to a few meters at night during low solar activity, with the satellite positioned at zenith angle (Bagiya et al., 2009). By measuring this delay using dual frequency GPS receivers, properties of the ionosphere can be inferred and used to monitor space weather events such as GNSS, HF communications, Space Based Observation Radar and Situational Awareness Radar, etc. It is documented that ionospheric delay which is proportional to TEC is the highest contributor to GPS positioning error (Alizadeh et al., 2013; Akala et al., 2013).

TEC in the ionosphere can also be studied using empirical ionospheric model such as the International Reference Ionosphere (IRI). IRI is a joint undertaking by the Committee on Space

Research (COSPAR) and International Union of Radio Science (URSI) with the goal of developing and improving an international standard for the parameters in earth's ionosphere (Bilitza et al., 2014). An updated version has been developed recently to cater for lapses of previous models. IRI provides the vertical TEC (VTEC) from the lower boundary (60 – 80 km) to a user-specific upper boundary (Bilitza et al., 2016).

In the past few decades, studies on the temporal and spatial variations of TEC have gained popularity in the scientific community (Wu et al., 2008). However, understanding the variability of TEC will also go a long way in obtaining the positioning accuracy of GNSS under disturbed and quiet conditions. The global distribution of TEC variations and its characteristics at all latitudes, during different solar cycle phases under disturbed and quiet conditions have been investigated by some researchers (Bhuyan and Borah, 2007; Maruyama et al., 2004; Jee et al., 2004).

Rama Rao et al. (2006a, b); Wanninger (1993) reported maximum day-to-day variability in TEC at the Equatorial Ionization Anomaly (EIA) crest regions, increasing peak value of TEC with increase in integrated equatorial electrojet (IEEJ) strength, maximum monthly average diurnal variations during equinox months followed by winter months and lowest during summer months. They also reported positive correlation of TEC and EEJ and the spatial variation of TEC in the equatorial region. Titheridge (1974) and Langley et al. (2002) attributed the lower TEC values during the summer seasons to low ionization density resulting from reduced O/ N₂ ratio (production rates) which is a result of increased scale height. Bhuyan and Borah (2007); Komjathy et al. (1998); Lee and Reinisch (2006) compared TEC derived from GPS receivers with IRI model in the equatorial/ low latitude sector and inferred that the diurnal amplitude of TEC is higher during the equinoxes followed by December solstices and lowest in June solstice, i.e., observing winter

anomaly in seasonal variation. They further reported discrepancies between IRI model and their measured values during most hours of the day at their various locations. Malik et al. (2016) reported higher IRI values than observed maximum useable frequency (MUF) values but behaves similarly diurnally and seasonally with no clear trend. Akala et al. (2013) on the comparison of equatorial GPS-TEC observations over an African station and an American station during the minimum and ascending phases of solar cycle 24 reported that seasonal VTEC values were maximum and minimum during March equinox and June solstice respectively, during minimum solar cycle phase at both stations. They also reported that during the ascending phase of solar cycle 24, minimum and maximum seasonal VTEC values were recorded during December solstice and June solstice respectively. They further showed that IRI-2007 model predicted better in the American sector than the African sector.

The aim of this paper is (i) to characterize TEC on diurnal, seasonal and solar cycle scales in the Nigerian Equatorial ionosphere (ii) to compare OBS-TEC with IRI-2016 model in order to find if the model underestimates or overestimates TEC values at the African longitudinal sectors.

2 DATA AND METHODOLOGY

2.1 DATA

The Receiver Independence Exchange (RINEX) Observation GPS data files were downloaded daily from NIGNET website (www.nignet.net) and processed using Bernese software and GPS TEC analysis software. The RINEX file contains 60 iteration data (i.e. in 1 minute time resolution). The GPS-TEC analysis software was designed by Gopi Seemala of the Indian Institute of Geomagnetism. The summary of this application is to read raw data, processes cycle slips in phase data, reads satellite biases from the International GNSS services (IGS) code files (and

calculates them if unavailable), and calculates receiver bias, inter-channel biases for different satellites in the constellation, and finally plots the VTEC values on the screen and writes the ASCII output files (*CMN) for STEC and (*STD) for VTEC in the same directory of the data files. Effect due to multipath is eliminated by using a minimum elevation angle of 50°.

Observation GPS-TEC obtained from the TEC analysis software is the slant TEC (STEC) and vertical TEC (VTEC). STEC is polluted with several biases that must be eliminated to get VTEC. VTEC is calculated from the daily values of STEC using Eq. (3).

$$VTEC = (STEC - [b_R + b_S + b_{RX}])/S(E) \quad (3)$$

Where b_R , b_S , and b_{RX} are receiver bias, satellite bias and receiver interchannel bias respectively. $S(E)$, which is the oblique factor with zenith angle, z at IPP (Ionospheric Pierce Point) is expressed in Eq. (4).

$$S(E) = \frac{1}{\cos(z)} = \left\{ 1 - \left(\frac{R_E \times \cos(E)}{R_E + h_S} \right)^2 \right\}^{-0.5} \quad \text{Bolaji et al. (2012)} \quad (4)$$

R_E = the mean radius of the earth in km and h_S = ionospheric height from the surface of the earth. According to Rama Rao et al., (2006c), ionospheric shell height of approximately 350km is appropriate for the equatorial/ low latitude region of the ionosphere for elevation cut off angle of > 50°. This is valid in this study.

Hourly VTEC data obtained from these processing software are averaged to daily TEC values in TEC units ($1 \text{ TECU} = 10^{16} \text{ el/m}^2$). OBS-TEC from Birnin-kebbi, on geographic Latitude 12.47° N and geographic Longitude 4.23° E located in Northern Nigeria, obtained during the period 2011 – 2014, which corresponds to the ascending (2011 – 2013) and maximum (2014) phases of solar cycle 24 were compared with derived TEC obtained from International Reference Ionosphere (IRI-2016) model website (https://ccmc.gsfc.nasa.gov/modelweb/models/iri2016_vitmo.php). The 2016 version of IRI

provides important changes and improvements on previous IRI versions (Bilitza et al., 2016). Solar cycle 24 is regarded as a quiet solar cycle which peaked in 2014 with maximum sunspot number (103) occurring in February. Values of sunspot number, R_z , in Text format were obtained from Space Physics Interactive Data Resource (SPIDR) website (www.ionosonde.spidr.com) before it became unavailable. Table 1 shows the years used in this study and their corresponding sunspot number, R_z .

Table I: Table of years, solar cycle phase and sunspot number, R_z [Source: Author].

Years	Solar Cycle Phase	Sunspot Number, R_z
2011	Ascending	55.7
2012	Ascending	57.6
2013	Ascending	64.7
2014	Maximum	79.6

2.2 METHODOLOGY

Diurnal variations of hourly OBS-TEC and hourly IRI-2016 model (NeQuick topside option) were plotted using the monthly mean values of OBS-TEC and monthly mean of IRI-2016 model against local time (LT) on the same Figure. The corresponding percentage deviation (percentage Dev or % DEV) of IRI-2016 from OBS-TEC were also analysed using the monthly mean values of OBS-TEC and monthly mean values of IRI-2016 against local time (LT). Percentage Dev is obtained using Eq. (5) below:

$$\%DEV = \left(\frac{OBS-IRI}{OBS} \right) \times 100 \quad (5)$$

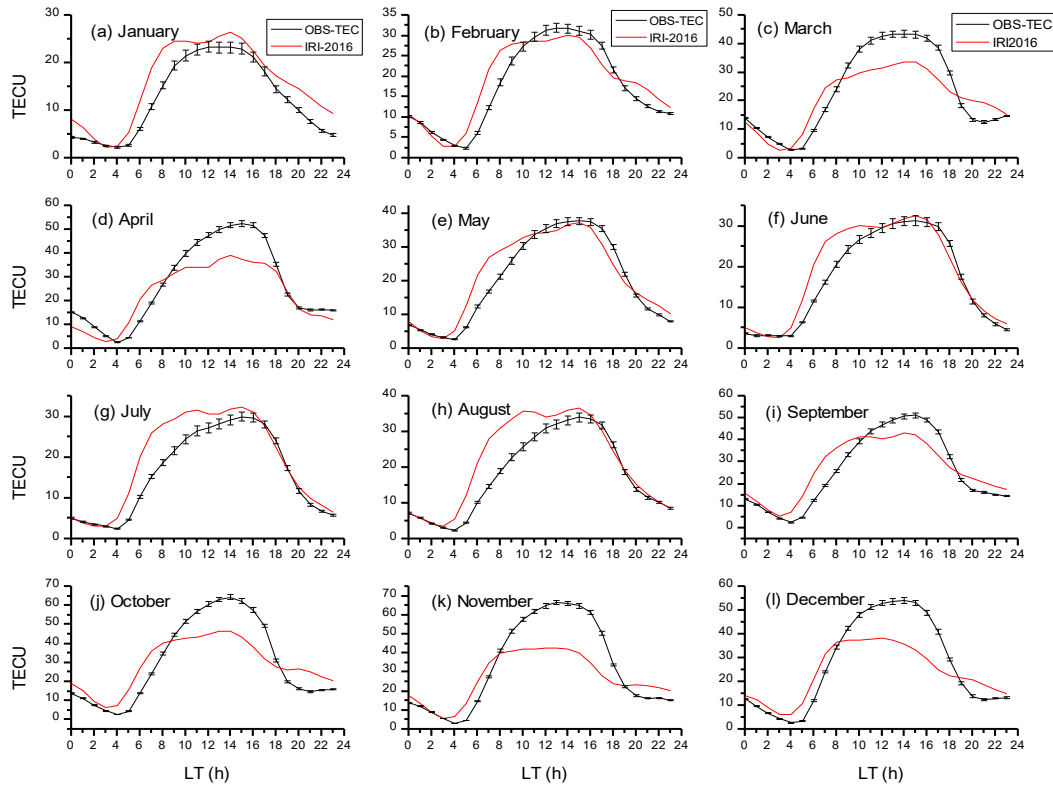
where OBS represents Observation-TEC values and IRI represents TEC derived by IRI-2016 model.

The OBS-TEC data was grouped following Onwumechilli and Ogbuehi (1964) into four seasons namely: March equinox (February, March and April), June solstice (May, June and July), September equinox (August, September and October) and December solstice (November, December and January), in order to investigate seasonal variation. Finally, Annual variation of OBS-TEC and sunspot number, R_z were also analysed by plotting mean OBS-TEC and mean R_z against each month of the year.

3 RESULT AND DISCUSSIONS

Figures 1 to 4 shows the diurnal variation of OBS-TEC and IRI-2016 model in the Nigerian Equatorial Ionosphere (NEI) for the years 2011 to 2014 respectively. OBS-TEC were obtained from the GPS receiver installed at Birnin-Kebbi station. The diurnal variation of OBS-TEC and IRI-2016 model TEC reveals the typical characteristics of an equatorial/ low latitude ionosphere. Generally, the day-to-day variation of OBS-TEC have been indicated using error bar showing the standard deviation from mean values. The study reveals that day-to-day variation of OBS-TEC is higher during the daytime than night time for all the years. It well known fact that during the day, the sun causes variations in temperature, neutral wind, electron density and electric field thereby modulating the structure and evolution of the ionosphere and thermosphere (Gorney, 1990; Forbes et al. (2006). These Figs. shows a steep rise in OBS-TEC from a minimum of ~2 TECU between 03:00 – 05:00 LT in 2011, ~3 TECU (04:00 – 05 LT) in 2012, ~3 TECU (03:00 – 05:00 LT) in 2013 and 2014. OBS-TEC increased to a broad daytime maximum between 12:00 LT – 14:00 LT for all years before falling to a minimum after sunset. The diurnal variation of IRI-2016 model shows TEC increasing from a minimum of ~ 2 TECU in 2011, ~ 4 TECU in 2012 and 2013, and

203 ~ 5 TECU in 2014 between 03:00 – 04:00 LT for all years, to a broad daytime peak between 08:00
 204 – 14:00 LT, before falling steeply to minimum before sunset. Hence the IRI-2016 model attained
 205 its peak before OBS-TEC. Dabas et al. (2003); Somoye et al. (2011); Hajra et al. (2016); D’ujanga
 206 et al. (2017) attributed the steep increase in TEC to solar EUV ionization and upward vertical $\mathbf{E} \times$
 207 \mathbf{B} resulting from the rapid filling up of the magnetic field tube at sunrise and meridional winds
 208 (Suranya et al., 2015). These magnetic field tubes collapse after sunset due to low thermospheric
 209 temperature and Rayleigh Taylor Instability (RTI) (Ayorinde et al., 2016) giving rise to the
 210 minimum TEC values after sunset. These results are similar to findings of Bolaji et al., (2012),
 211 Fayose et al., (2012), Okoh et al., (2014), Eyelade et al., (2017) who have explored the NEI.



212 Fig. 1: Diurnal variation of OBS-TEC showing error bar and IRI-2016 model of each month during
 213 January – December 2011 at Birnin-Kebbi

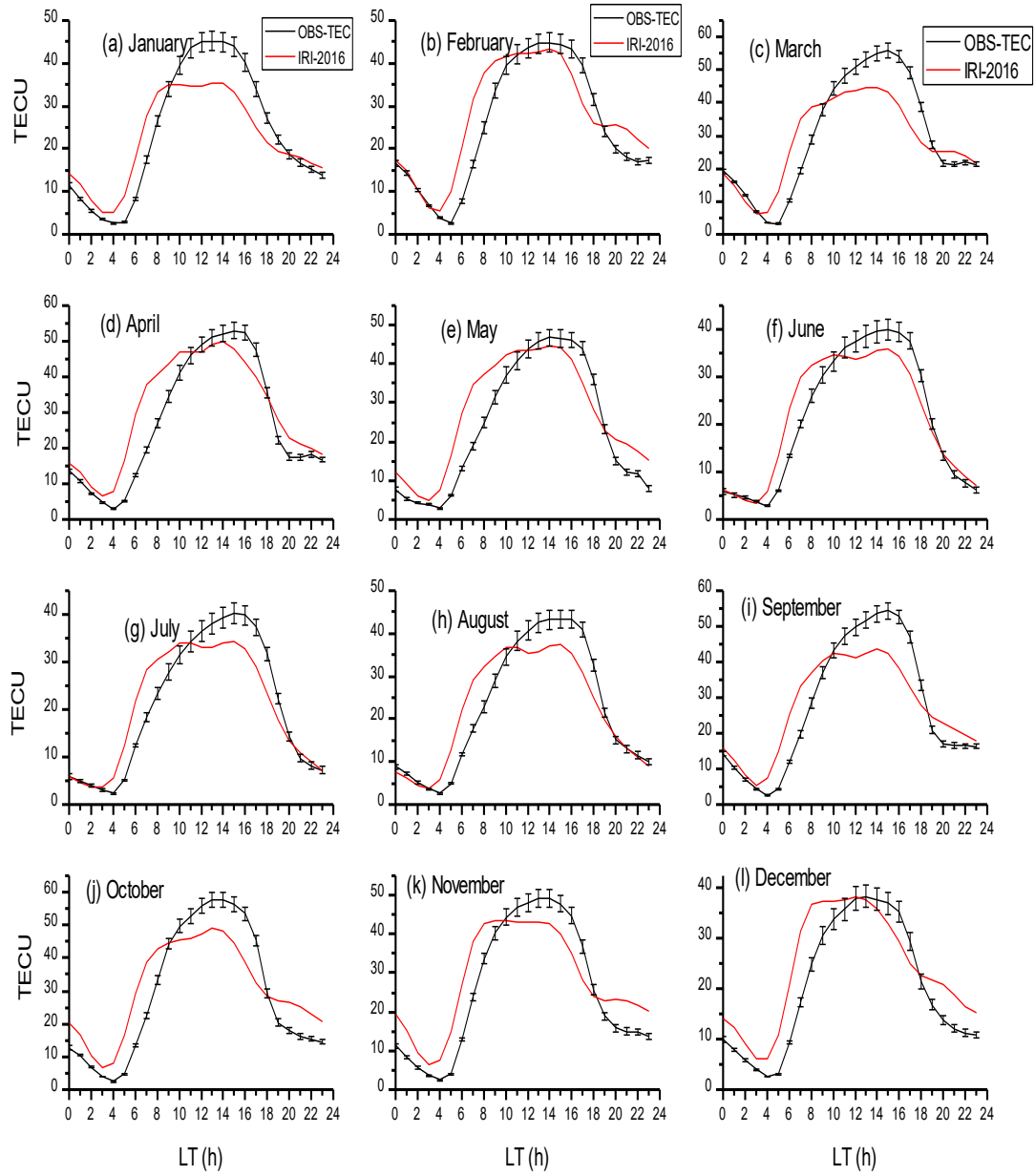


Fig. 2: Same as Figure 1 for 2012.

214

215

216

217

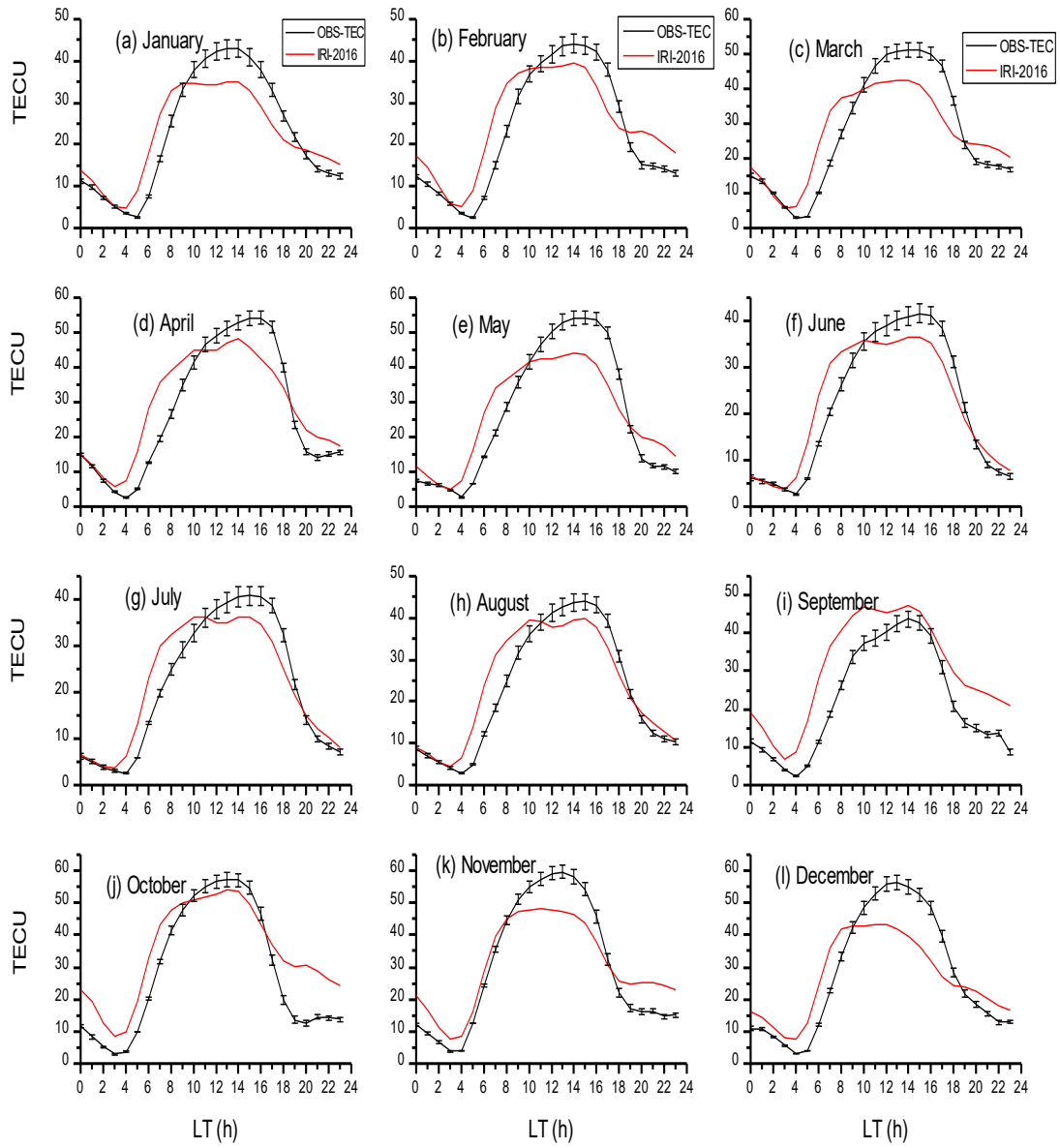


Fig. 3: Same as Figure 1 for 2013.

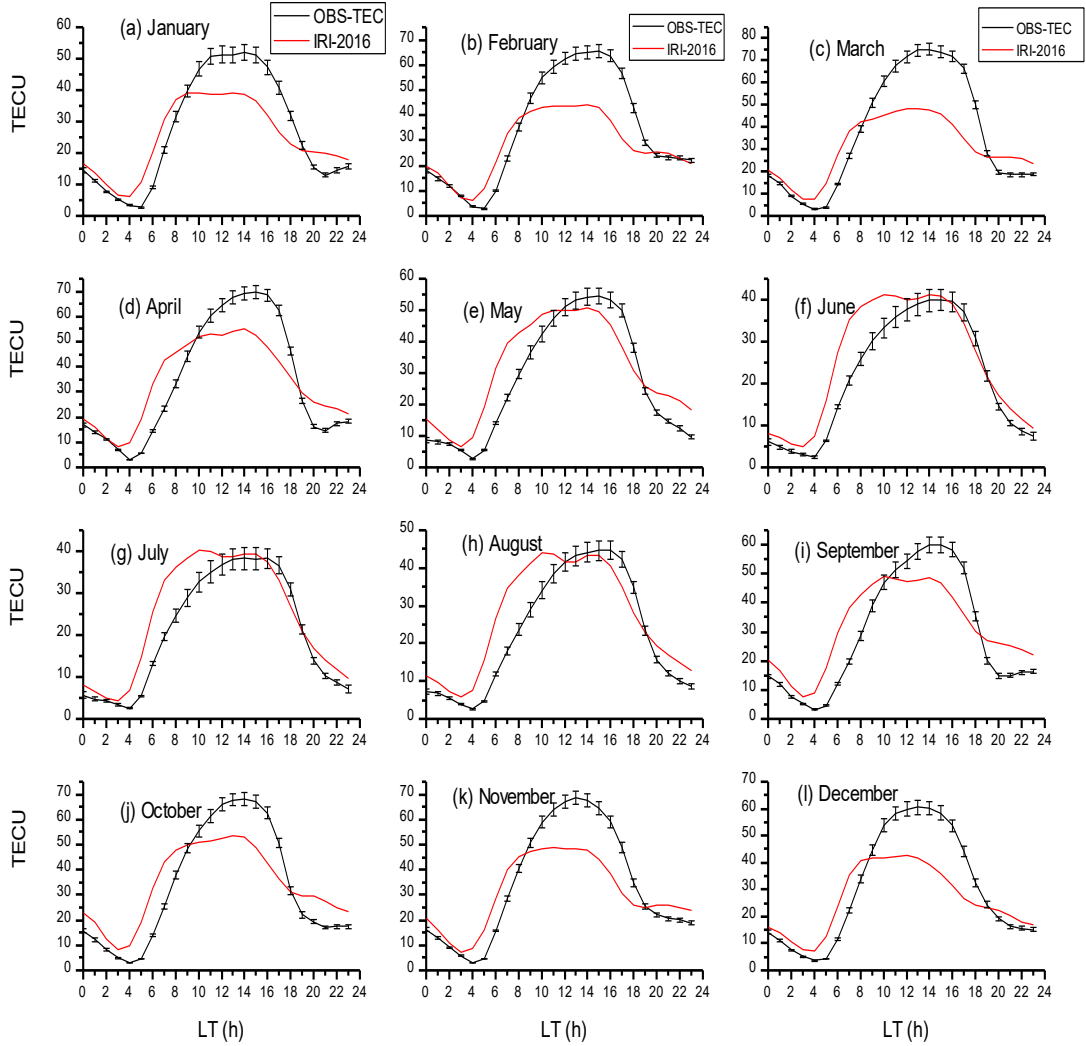


Fig. 4: Same as Figure 1 for 2014.

It can be seen that OBS-TEC is much higher in 2014 with maximum value up to 70 TECU in March compared with IRI-2016 maximum of 54 TECU in the month of October, 2014. The diurnal variation reveals that the peak of OBS-TEC of majority of the months for all years shifted to slightly post-noon hours (13:00 – 14:00 LT). This type of peak shifting is peculiar to equatorial/ low latitude regions and the Polar Regions of the ionosphere and it is found to depend on the equatorial ionization anomaly and solar zenith angle respectively (Rama Rao et al., 2009; D’ujanga

et al., 2017). Another major phenomenon seen in the diurnal variation of OBS-TEC is the post-sunset decrease and slight enhancement in some months. The night time enhancement of TEC, for example, March, April and October of the year 2011, March and April of the year 2012, March, April, September and October of the year 2013, January, April and September of the year 2014 was documented by previous researchers like Rama Rao et al., 2009; D’ujanga et al., 2017. They attributed it to the product of eastward and westward directed electric field which produces an upward and downward motion of ionospheric plasma during the day and night respectively.

Figures 5 to 8 shows the diurnal variation of percentage deviation of IRI-2016 model from OBS-TEC in the Nigerian Equatorial Ionosphere (NEI) for all years respectively. On a general note, IRI-2016 model only presented suitable predictions for the post-midnight hour between 00 – 03 LT of the day for all years. All other hours from 04 – 23 LT shows some discrepancies. In some months, these discrepancies lasted throughout the day for example, in the months of October, November and December of 2012, October and December, 2013, and September and October of 2014, while in some other months these discrepancies collapsed during the pre-midnight hours (18 – 23 h), for example, in the months of June, July and August of 2011, June, July and August of 2012, June and August of 2013 and February, June and July of 2014. It is also important to mention that IRI-2016 model either over estimated or under estimated TEC in the NEI especially during daytime hours as shown in the plots.

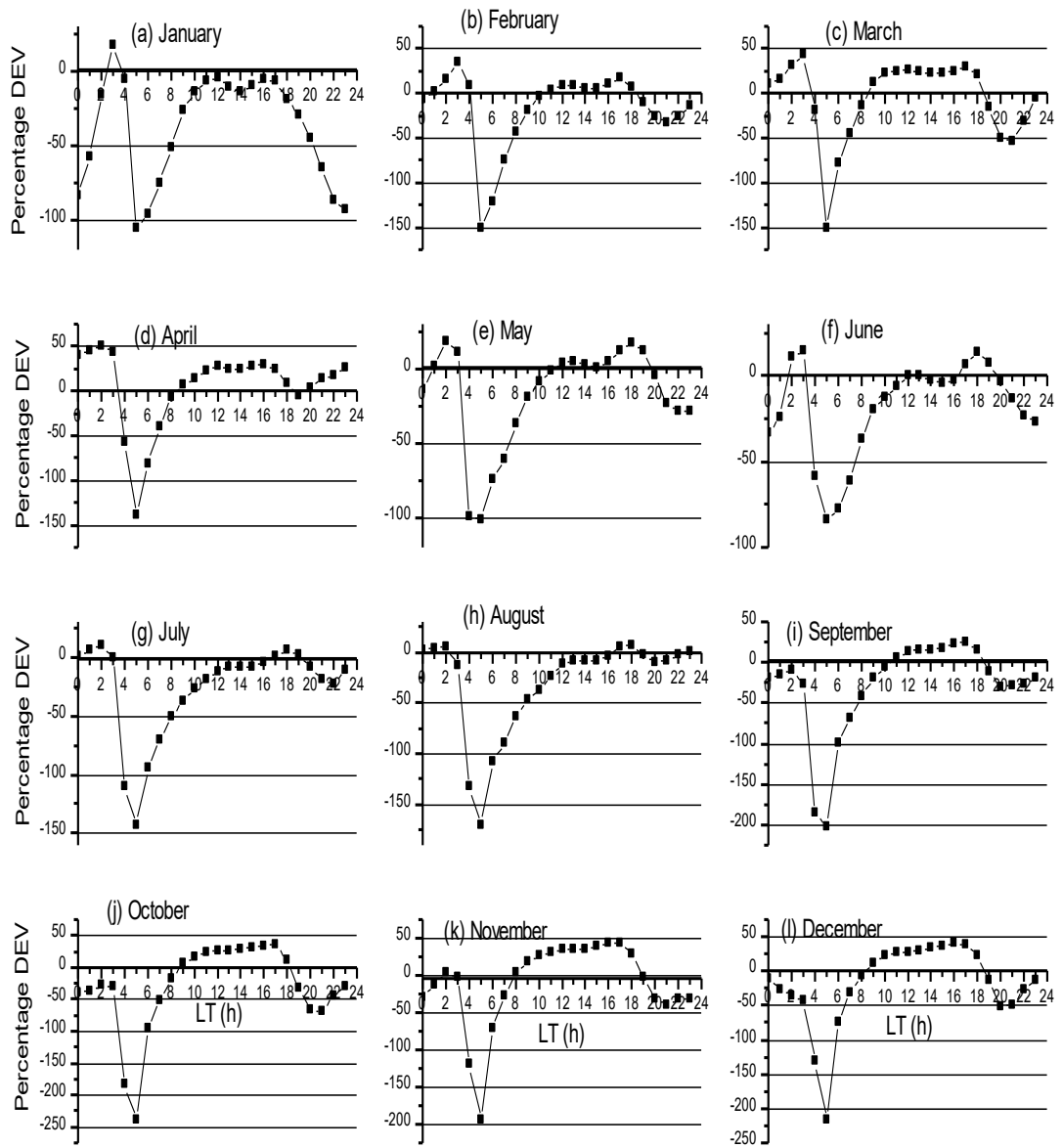


Fig. 5: Percentage deviation of IRI-2016 from OBS-TEC for year 2011

252

253

254

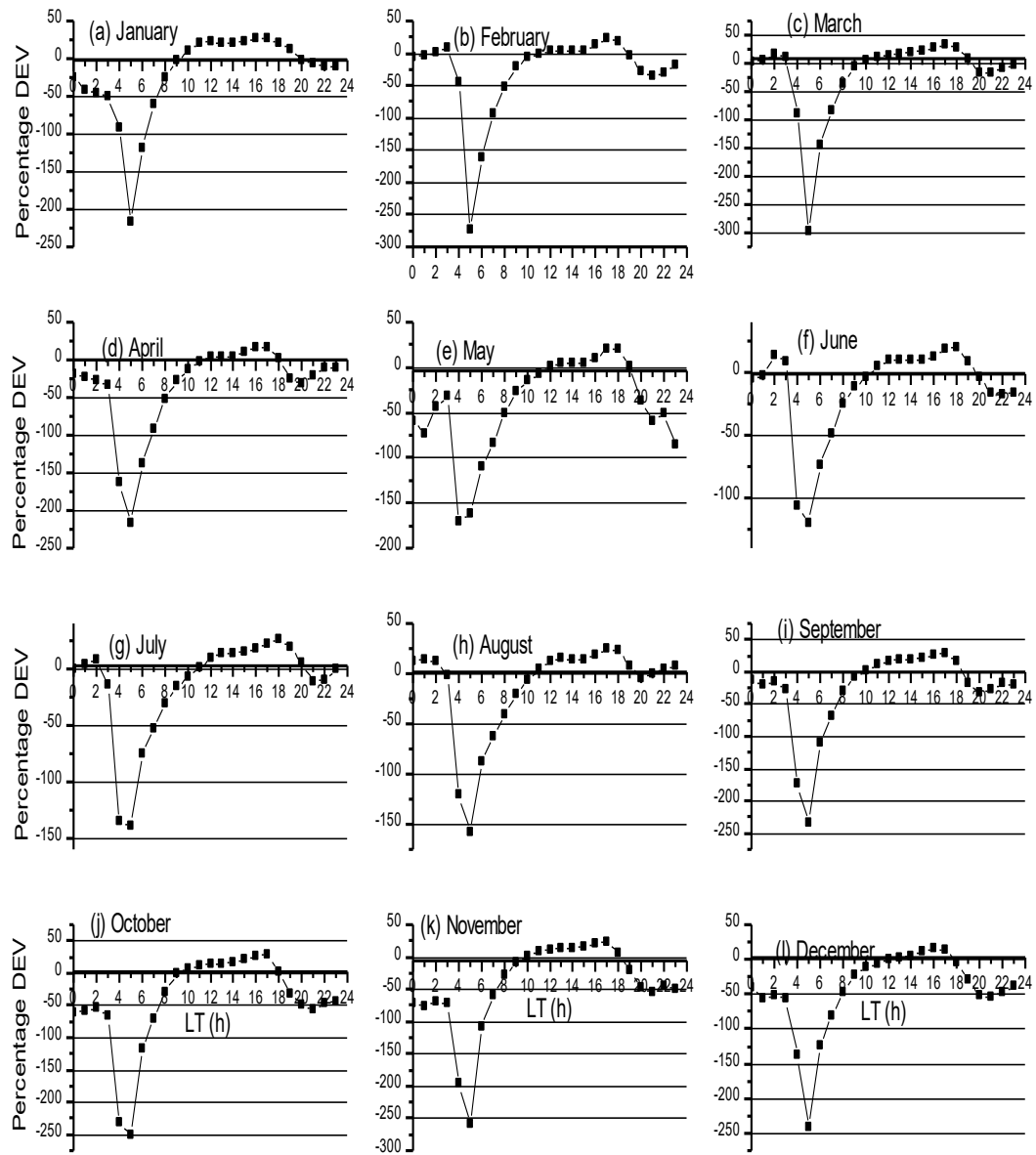


Fig. 6: Percentage deviation of IRI-2016 from OBS-TEC for year 2012

255

256

257

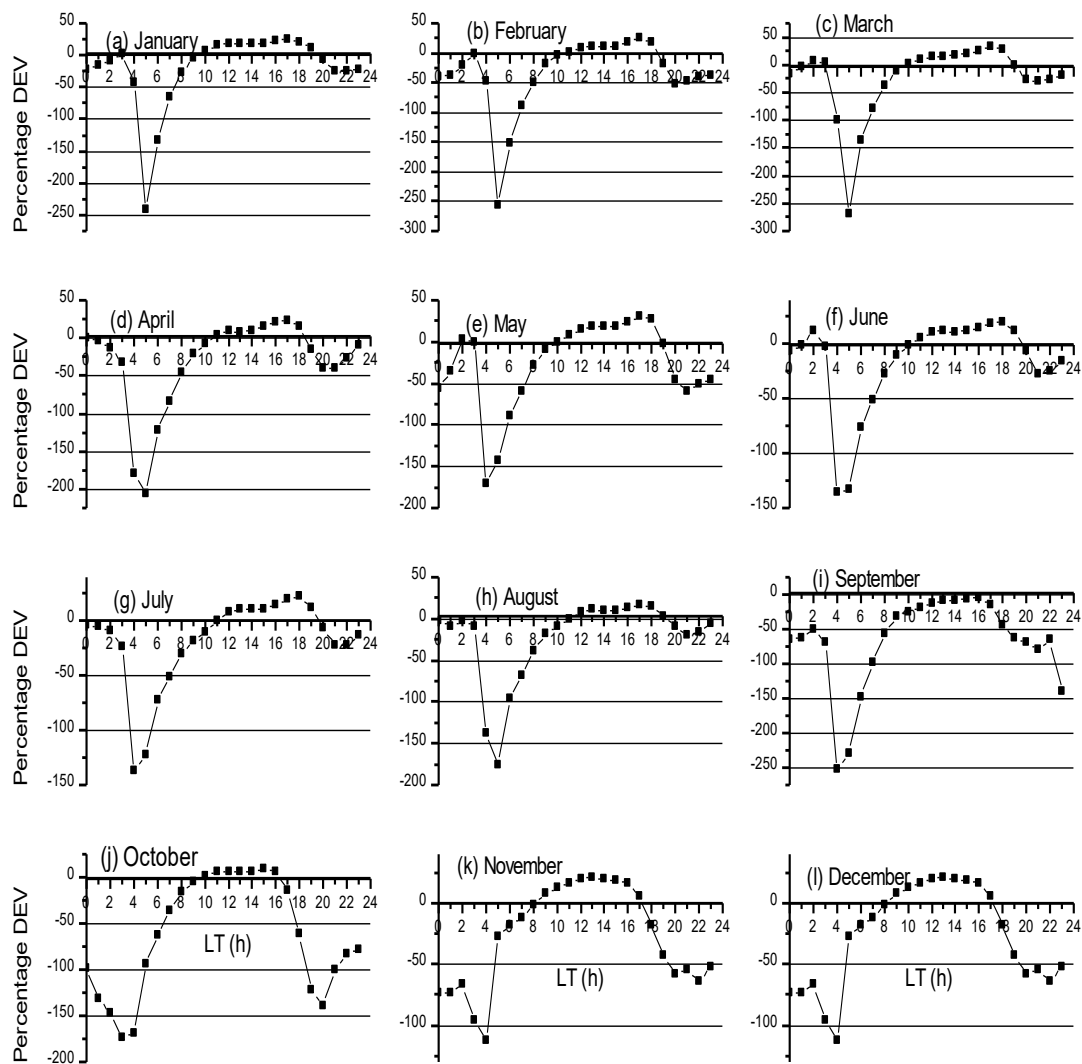


Fig. 7: Percentage deviation of IRI-2016 from OBS-TEC for year 2013

258

259

260

261

262

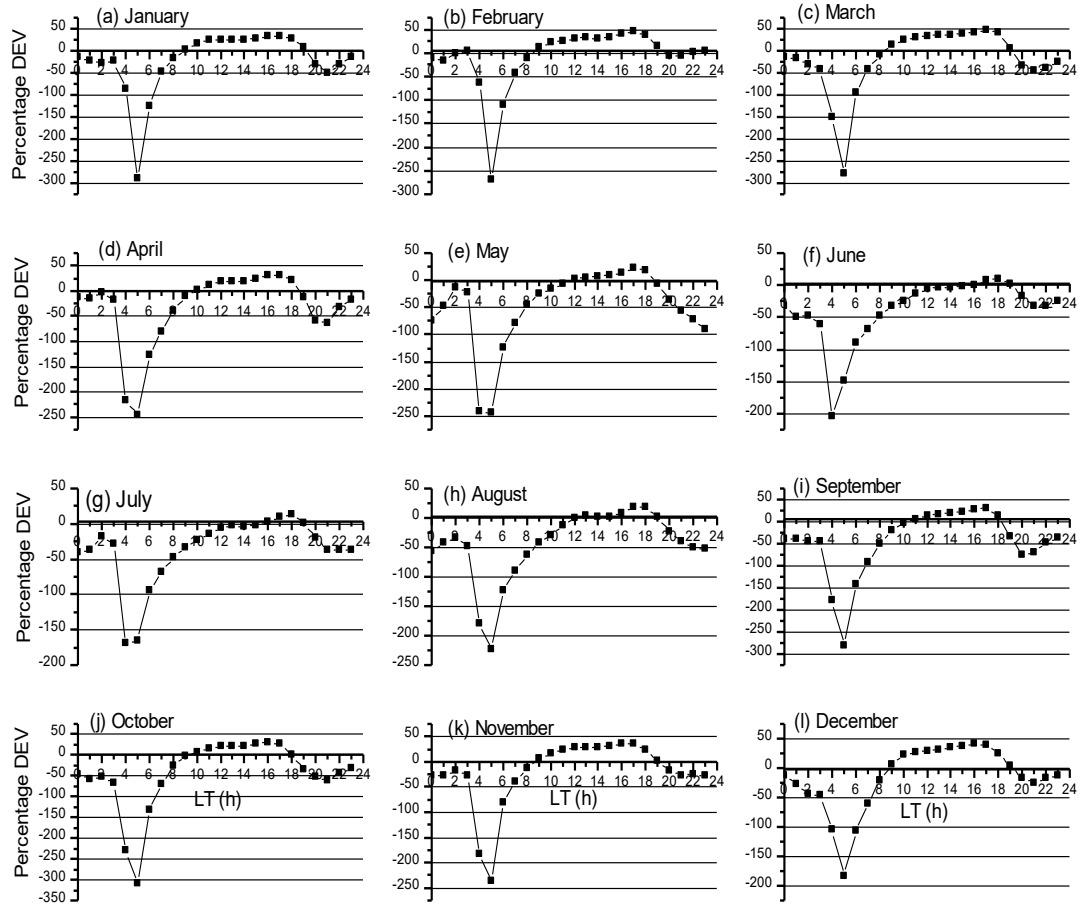


Fig. 8: Percentage deviation of IRI-2016 from OBS-TEC for year 2014

The mass plots in the Figs. 5 - 8 further reveal that negative percentage deviation shows higher values of IRI-2016 than OBS-TEC values. The reverse is the case for positive percentage deviation. Highest negative percentage deviations are seen between 04 – 05 LT for all months throughout the years in this study. Highest Negative percentage deviation of ~ 300% was recorded in the month of October, 2014 at 05 LT. Table II shows the summary of months with daytime over- or under-estimate of IRI-2016 in the NEI.

Table II: Months of daytime estimate of IRI-2016 model in NEI [Source: Author]

YEAR	OVER ESTIMATE	UNDER ESTIMATE	SAME RANGE
2011	January, July, August	February – April, September - December	May - June
2012		January - December	
2013	September	January – August, October - December	
2014		January - December	

Therefore, it is clear from the Figs. 1- 4, Figs. 5 – 8 and Table II that IRI-2016 model did not predict well in the NEI. This may be attributed to insufficient data which is as a result of the sparse distribution of GPS infrastructure in this region. Our result agree with those Komjathy et al. (1998); Lee and Reinisch (2006); Malik et al. (2016). Bhuyan and Borah (2007) reported higher IRI TEC than their measured values at about all local time in their location. Mosert et al. (2007) and Sethi et al. (2010) also reported discrepancies between of IRI TEC predictions and GPS TEC during high solar activity (HSA) and low solar activity (LSA) respectively at equatorial/ low latitudes.

Figure 9 show plots the seasonal variations of OBS-TEC for the four years under investigation. The change in concentration of Oxygen and molecular Nitrogen has been reported to be the main cause of seasonal variation of ionospheric parameters. Seasonal variation of OBS-TEC in this study depicts semi-annual variation with equinoctial maximum (~ 52 TECU) and solsticial minimum (~ 44 TECU) in 2012. D’ujanga et al., (2017) reported that since the sun passes through the equator during the equinox, both March and September equinox experience the same

solar radiation. It is also a well-established fact that March 20 and September 23 are the only times in the year when the solar terminator is perpendicular to the equator, giving rise to the equinoctial maximum. The semi-annual variation resulting from the effect of equatorial ionization anomaly (EIA) in the ionosphere has been attributed to the effect of solar zenith angle and magnetic field geometry (Wu et al., 2008; Rama Rao et al., 2006a). Another important feature of ionospheric parameters (known as equinoctial asymmetry) which is reported in the work of Bolaji et al., (2012); Akala et al., (2013); Eyelade et al., (2017); D'ujanga et al., (2017); Aggarwal et al., (2017), is clearly seen in all years used in this work. Akala et al., (2013) also reported **minimum and maximum seasonal VTEC values during June solstice and December solstice respectively**, during ascending phase of solar cycle 24. Equinoctial asymmetry is a strong phenomenon in low latitudes (Aggarwal et al., 2017). The equinoctial asymmetry has been explained in terms of the differences in the meridional winds leading to changes in the neutral gas composition during the equinoxes.

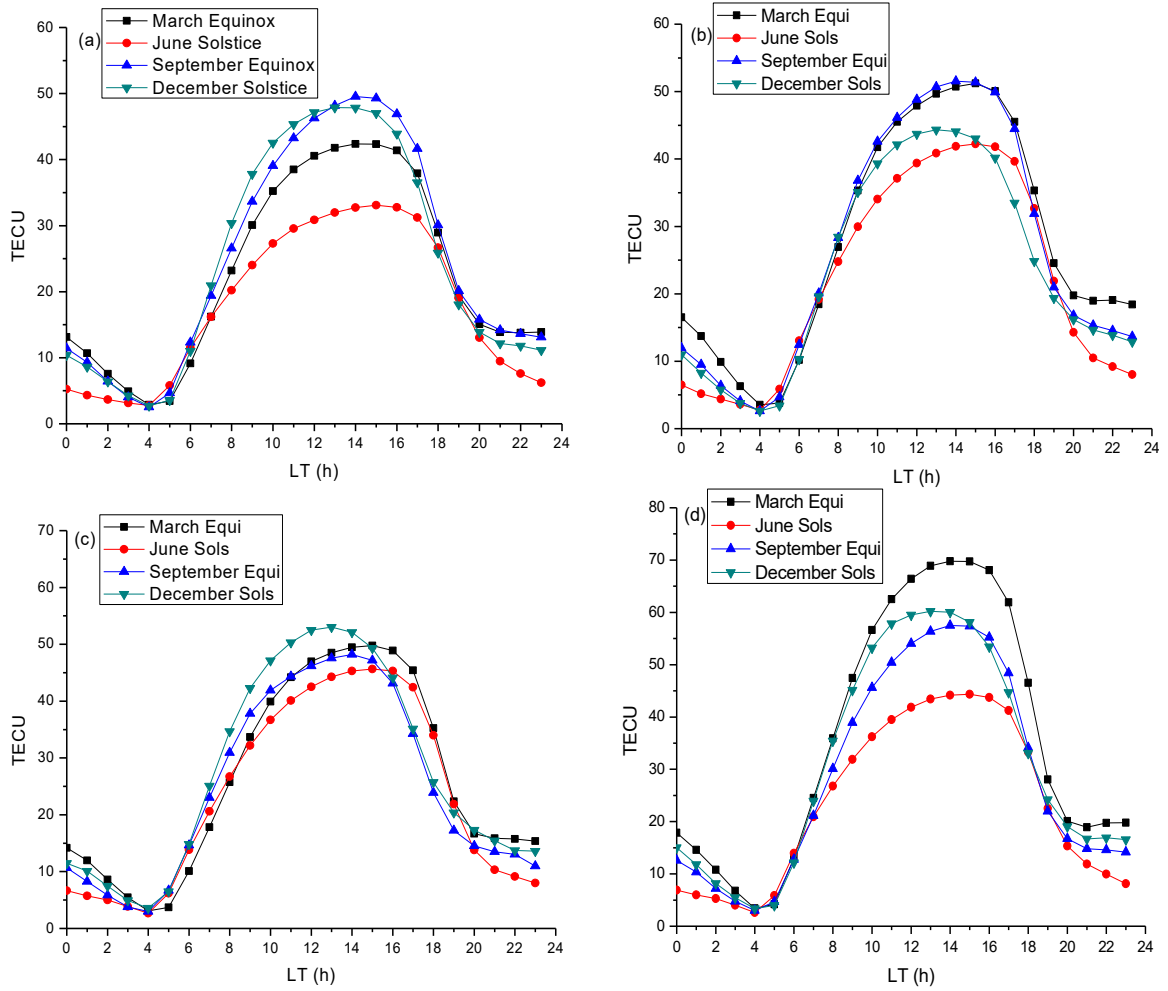


Fig. 9: Seasonal variation of observed OBS-TEC during (a) 2011 (b) 2012 (c) 2013 and (d) 2014

In 2011 and 2014, the seasonal variation of OBS-TEC in the ionosphere did not follow the pattern reported by these researchers. In 2011, September equinox and December solstice recorded higher magnitude, followed by March equinox; the lowest was in June solstice. In 2013, December solstice magnitude was highest, followed by the equinoxes, March and September respectively and lowest in June solstice. This corresponds to result obtained by Akala et al. (2013), which they attributed to increase in ion production rate in winter season and anti-correlation between December and June Solstice pre-reversal velocity enhancement. In 2014, March equinox and

December solstice magnitudes were higher than September equinox and June solstice magnitudes. December solstice magnitude is found to occur between the magnitudes of the equinoxes in 2011 and 2014. The September equinox magnitude and March equinox magnitude are observed to interchange in 2011 and 2014. Overall, June solstice magnitudes were lowest during all the years. This is due to low ionization resulting from reduced production rates, i.e. O/ N₂ ratio (Titheridge 1974).

Also, for all seasons, pre-midnight (18 – 23 LT) values of TEC are higher than post-midnight (00 – 05 LT) TEC values for all years. In 2011, pre- midnight TEC values are in the range of 8 – 30 TECU while post-midnight TEC values ranges from 3 to 13 TECU. In 2012, pre-midnight TEC values are in the range of 9 – 35 TECU while post-midnight TEC values are between 3 to 17 TECU. In 2013, the pre-midnight TEC values are between 9 – 35 TECU while post-midnight TEC values ranges from 3 – 15 TECU. Finally in 2014, pre-midnight TEC values are between 9 to 47 TECU while the post-midnight TEC ranges from 3 to 18 TECU. Furthermore, the maximum OBS-TEC values in 2011 (49 TECU) and 2012 (52 TECU) were recorded in September Equinox season. In 2013, OBS-TEC reached a maximum of 53 TECU in December solstice while in 2014, the maximum OBS-TEC (70 TECU) was recorded in March Equinox season. This result agrees in general with those of D’ujanga et al. (2017) who obtained higher TEC values during the equinoxes than during the solstices. This same result was observed by Bagiya et al. (2009) that TEC values are high in equinoctial months than solstitial months. Seasonal variation of TEC is dependent on thermospheric neutral compositions since during the day the equator is hotter than the pole. Meridional winds therefore flows from the equator towards the pole. This flow cause a change in the neutral composition resulting in the decrease of the ratio of O/ N₂ at the equator. The decrease which is maximum at the equinox result in higher TEC values at the equinox (Bagiya et

al., 2009). The corresponding annual range error (meters) of the season with maximum OBS-TEC using 1 TECU variation to represent an error of 0.16 m in position is summarized in Tables III.

Table III: Season of maximum OBS-TEC and their corresponding range error.

YEAR	SEASON OF MAXIMUM OBS-TEC	VALUE (TECU)	CORRESPONDING ERROR (m)
2011	September Equinox	49	8
2012	September Equinox	52	8
2013	December Solstice	53	8
2014	March Equinox	70	11

Figure 10 shows the comparison of the monthly OBS-TEC and sunspot number, R_z from 2011 – 2014, showing an increase of TEC with solar cycle. Our result is in good agreement with those of Chakrabarty et al. (2012) and D’ujanga et al. (2017). The former authors reported a direct solar effect on TEC while the latter authors observed that the trend in TEC follow that of solar parameters. The present result also agrees with that of Rama Rao et al. (1985) who reported a direct solar control on TEC. Ionospheric climatology especially solar activity and the equatorial ionization anomaly (EIA) effects of the ionosphere provides an insight into space weather events (Liu et al., 2011).

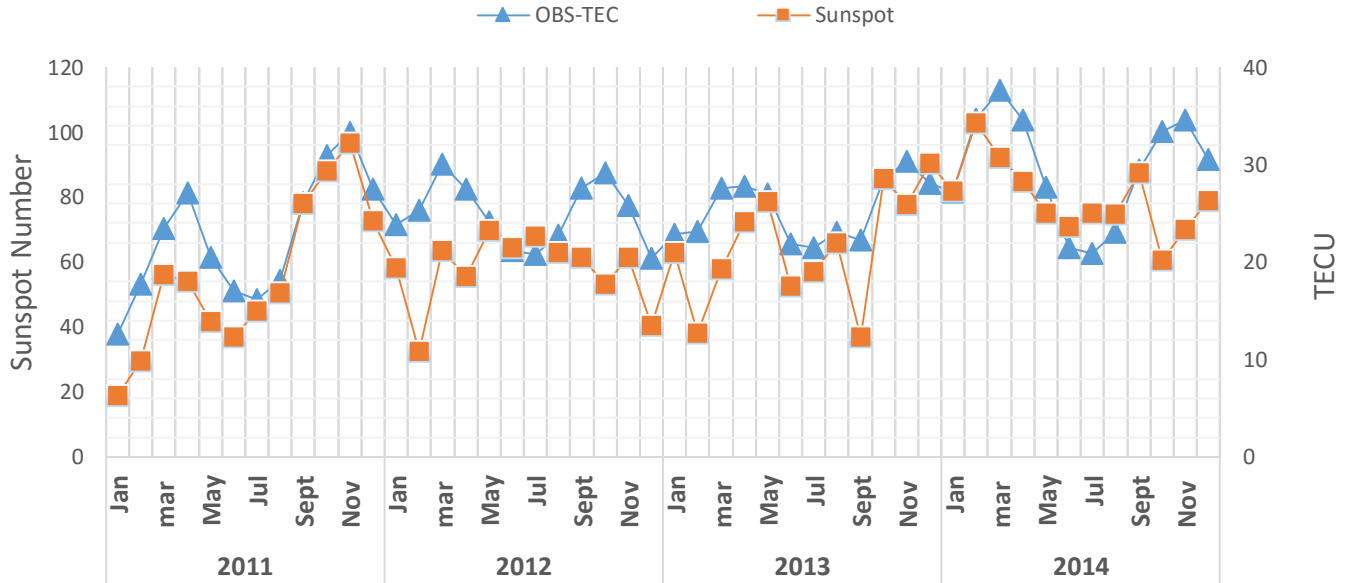


Fig. 10: Annual variation of OBS-TEC and sunspot number, Rz

4 CONCLUSIONS

Studies on OBS-TEC and IRI-2016 model at Birnin-Kebbi in Northern Nigeria during the ascending and maximum phases of solar cycle 24 have been carried out. The result obtained reveals the following:

1. Day-to-day variations of TEC were observed to be higher during the daytime than nighttime for all the years. During the day, the sun causes variations in temperature, neutral wind, electron density and electric field in the ionosphere. The diurnal variation shows a steep rise in OBS-TEC from a minimum of ~2 TECU between 03:00 – 05:00 LT in 2011, ~3 TECU (04:00 – 05 LT) in 2012, ~3 TECU (03:00 – 05:00 LT) in 2013 and 2014. OBS-TEC increased to a broad daytime maximum between 12:00 LT – 14:00 LT for all years before falling to a minimum after sunset. Magnetic field tubes are rapidly filled up at dawn resulting in the increase of extreme ultraviolet (EUV) ionization (Anderson et al., 2004;

D’ujanga et al., 2017). The diurnal variation of IRI-2016 model shows TEC rising from a minimum of ~ 2 TECU in 2011, ~ 4 TECU in 2012 and 2013, and ~ 5 TECU in 2014 between 03:00 – 04:00 LT, to a broad daytime peak between 08:00 – 14:00 LT, before falling to a minimum before sunset.

2. The diurnal variation reveals that the peak of OBS-TEC of some months were delayed till after-noon. Post-sunset decrease and enhancement due to pre-reversal zonal electric field after sunset, were also observed in the diurnal variation of OBS-TEC in some months.
3. On a general note, it can be concluded that IRI-2016 model and OBS-TEC show some discrepancies throughout the day except during the post-midnight hours (00 – 05 LT) in the NEI.
4. For all seasons, pre-midnight (18 – 23 h) values of TEC are higher than post-midnight (00 – 05 h) TEC values during all years. In 2011, pre- midnight TEC values are in the range of 8 – 30 TECU while post-midnight TEC values ranges from 3 to 13 TECU. In 2012, pre-midnight TEC values are in the range of 9 – 35 TECU while post-midnight TEC values are between 3 to 17 TECU. In 2013, the pre-midnight TEC values are between 9 – 35 TECU while post-midnight TEC values ranges from 3 – 15 TECU. Finally in 2014, pre-midnight TEC values are between 9 to 47 TECU while the post-midnight TEC ranges from 3 to 18 TECU.
5. Maximum OBS-TEC values in 2011 (49 TECU) and 2012 (52 TECU) were recorded in September Equinox season. In 2013, OBS-TEC reached a maximum of 53 TECU in December solstice while in 2014, the maximum OBS-TEC (70 TECU) was recorded in March Equinox season. This result agrees in general with those of D’ujanga et al. (2017) and Bagiya et al. (2009) who obtained higher TEC values during the equinoxes than during

the solstices. Seasonal variation of TEC is dependent on thermospheric neutral compositions since during the day the equator is hotter than the poles.

6. Finally, annual variation of OBS-TEC and sunspot number, R_z reveal the strong dependence of TEC on solar activity (sunspot number). Solar activity and the equatorial ionization anomaly (EIA) effects of the ionosphere provides an insight into space weather events. OBS-TEC and sunspot number were found to increase gradually from 2011 to 2014. Rama Rao et al. (1985) reported a direct solar control on TEC.

AUTHORS' CONTRIBUTIONS

Author AA designed the study, obtained the data and wrote the first draft of the manuscript. Author BB and CC analysed the data and wrote the protocol. All other authors managed the literature searches, read and approved the final manuscript.

ACKNOWLEDGEMENT

We thank the Office of the Surveyor General of the Federation (OSGoF) for making TEC data available through the infrastructure www.nignet.net. We also thank Hatanaka, Y., Gopi Krishna for providing TEC processing software online. Finally, we appreciate Bilitza et al. (2017) for making the latest version of IRI model available online.

REFERENCES

Aggarwal, M., Bardhan, A., Sharma, D.K. Equinoctial asymmetry in ionosphere over Indian region during 2006 – 2013 using COSMIC measurements. *Advances in Space Res.*, 60, 999 – 1014, 2017.

407 Akala, A.O., Somoye, E.O, Adeloye, A.B., Rabiou, A.B. Ionospheric f_oF_2 variability at equatorial
 408 and low latitudes during high, moderate and low solar activity. Indian Journal of Radio and Space
 409 Physics.Vol. 40, 124 – 129, 2011.

410 Akala, A.O., Seemala, G.K., Doherty, P.H., Valladares, C.E., Carrano, C.S., Espinoza, J., and
 411 Oluyo, K.S. Comparison of equatorial GPS-TEC observations over an African station and an
 412 American station during the minimum and ascending phases of solar cycle 24. Ann. Geophys., 31,
 413 2085, 2013.

414 Alizadeh, M.M., Wijaya, D.D., Hobiger, T., Weber, R., Schuh, H. Ionospheric effects on
 415 microwave signals in J. Bohm and H. Schuh (eds). Atmospheric Effect in Space Geodesy. Springer
 416 atmospheric sciences. Doi: 10.1007/978-3-642-36932-2_2, © Springer-Verlag Berlin Heidelberg,
 417 2013.

418 Anderson, D., Anghel, A., Chau, J., Veliz, O. Daytime vertical $\mathbf{E} \times \mathbf{B}$ drift velocities inferred from
 419 ground-based magnetometer observations at low latitudes, Space Weather, 2, S11001; doi:
 420 10.1029/2004SW000095, 2004.

421 Ayorinde, T.T., Rabiou, A.B., and Amory-Mazaudier, C. Inter-hourly variability of Total Electron
 422 Content during the quiet condition over Nigeria within the Equatorial Ionization Anomaly region.
 423 J. Atmos. Solar Terr. Phys., 145, 21 – 33, 2016.

424 Bagiya, M.S., Joshi, H.P., Iyer, K.N., Aggarwal, M., Ravin-dran, S., and Pathan, B.M. TEC
 425 variations during low solar activity period (2005 – 2007) near the Equatorial Ionization Anomaly
 426 Crest region in India. Ann Geophys., 27, 1047 – 1057, 2009.

427 Bhuyan, P.K. and Borah, R.R. TEC derived from GPS network in India and comparison with the
 428 IRI. Advances in Space Res., 39, 830 – 840, 2007.

429 Bilitza, D., Altadill, D., Zhang, Y., Mertens, C., Truhlik, V., Richards, P., McKinnell, L.A.,
 430 Reinisch, B. International reference ionosphere 2012 – A model of international collaboration. J.
 431 Space Weather Space Clim., 4, 1 – 12, doi: 10.1002/201JA018009, 2014.

432 Bilitza, D., Altadill, D., Truhlik, V., Shubin, V., Galkin, I., Reinisch, B., and Huang, X.
 433 International reference ionosphere 2016: from ionospheric climate to real-time weather
 434 predictions. Space weather, 15, 418 – 429, doi: 10.1002/20165SW001593, 2016.

435 Bolaji, O. S., Adeniyi, J.O., Radicella, S.M., and Doherty, P.H. Variability of total electron content
 436 over an equatorial West African station during low solar activity. Radio Sci., 47, RS1001, doi:
 437 10.1029/2011RS004812, 2012.

438 Chakrabarty, D., Bagiya, M.S., Thampi, S.V., Iyer, K.N. Solar EUV flux (0.1 – 50 nm), $F_{10.7}$ cm
 439 flux, sunspot number and total electron content in the crest region of the ionization anomaly during
 440 the deep minimum between solar cycle 23 and 24. Indian Radio and Space Phys., 41, 110 – 120,
 441 2012.

442 Ciruolo, L., and Spalla, P. TEC analysis of IRI simulated data. Adv. Space Res., 29, 6, 959 – 966,
 443 2002.

444 Codrescu, M. V., Palo, S. E., Zhang, X., Fuller-Rowell, T. J., Poppe, C. TEC climatology derived
 445 from TOPEX/POSEIDON measurements, Journal of Atmospheric Solution, 61, 281-298, 1999.

446 Dabas, R.S., Singh, L., Lakshmi, D.R., Subramanyam, P., Chopra, P., Garg, S.C. Evolution and
 447 dynamics of equatorial plasma bubbles: relationships to $\mathbf{E} \times \mathbf{B}$ drifts, post-sunset total electron
 448 content enhancements, and equatorial electrojet strength. Radio Sci., 38, doi:
 449 10.1029/2001RS002586, 2003.

450 D'ujanga, F.M., Opio, P. Twinomugisha, F. Variation of total electron content with solar activity
 451 during the ascending phase of solar cycle 24 observed at Makerere University, Kampala. Space
 452 Weather: Longitude and Hemispheric Dependences and Lower Atmosphere Forcing, Geophysical
 453 Monograph 220, First Edition. Edited by Timothy Fuller-Rowell, Endawoke Yizengaw, Patricia
 454 H. Doherty, and Sunanda Basu. © 2017 American Geophysical Union. Published 2017 by John
 455 Wiley & Sons, Inc., 2017.

456 Eyelade, V.A., Adewale, A.O., Akala, A.O., Bolaji, O.S. and Rabi, A.B. Studying the variability
 457 in the diurnal and seasonal variations in GPS TEC over Nigeria. Ann. Geophys., 35, 701 – 710,
 458 2017.

459 Fayose, R.S., Rabi, B., Oladosu, O., Groves, K. Variation of total electron content (TEC) and
 460 their effect on GNSS over Akure. Nigeria, Applied Physics Research, 4, 2, 2012.

461 Forbes, J.M., Bruinsma, S., Lemoine, F.G. Solar rotation effects in the thermospheres of Mars
 462 and Earth. Science, 312, 1366–1368, 2006.

463 Gorney, D. J. Solar cycle effects on the near-earth space environment. Rev Geophys, 28, 315–
 464 336, 1990.

465 Hajra, R., Chakraborty, S.K., Tsurutani, B.T., DasGupta, A., Echer, E., Brum, C.G.M., Gonzalez,
 466 W.D., Sobral, H.A. An empirical model of ionospheric total electron content (TEC) near the crest
 467 of the equatorial ionization anomaly (EIA). J. Space Weather Space Clim., 6, A29, doi:
 468 10.1051/swsc/2016023, 2016.

469 Liu, L., Wang, W., Chen, Y., Le, H. solar activity effects on the ionosphere: A brief review. Space
 470 Physics and Space Weather Geophysics. Chinese science Bulletin. 56, 12, 1202 – 1211, 2011.

471 Jee, G., Schunk, R. W., Scherliess, L. Analysis of TEC data from the TOPEX/Poseidon mission,
 472 Journal of Geophysical Research, 109, A01301, doi:10.1029/2003JA010058, 2004.

473 Komjathy, A., Langley, R., Bilitza, D. ingesting GPS-derived data into the IRI for single frequency
 474 radar altimeter ionospheric delay corrections. Adv. Space Res., 22, 6, 793 – 802, 1998.

475 Langley, R., Fedrizzi, M., Paula, E., Santos, M., Komjathy, A. Mapping the low latitude
 476 ionosphere with GPS. GPS World, 13, 2, 41 – 46, 2002.

477 Lee, C.C. and Reinisch, B.W. Quiet condition hmF2, NmF2 and Bo variations at Jicamarca and
 478 comparison with IRI-2001 during solar maximum. J. Atmos. Solar Terr. Phys., 68, 2138 – 2146,
 479 2006.

480 Maruyama, T., Ma, G., and Nakamura, M. Signature of TEC storm on 6 November 2001 derived
 481 from dense GPS receiver network and ionosonde chain over Japan. Journal of Geophysical
 482 Research, 109, A10302, doi: 10.1029/2004JA010451, 2004.

483 Mosert, M., Gende, M., Brunini, C., Ezquer, R. and Altadill, D. Comparisons of IRI TEC with
 484 GPS and Digisonde measurements at Ebro. Advances in Space Res., 39, 841 – 847, 2007.

485 Okoh, D., Lee-Anne McKinnell, L., Cilliers, P., Okere, B., Okonkwo, C., Rabi, A.B. IRI-VTEC
 486 versus GPS-vTEC for Nigerian SCINDA GPS stations. Advances in Space Research,
 487 <http://dx.doi.org/10.1016/j.asr.2014.06.037>, 2014.

488 Ogunmodimu, O., Rogers, N.C., Falayi, E., Bolaji, S. Solar Flare induced cosmic noise absorption,
 489 NRIAG Journal of Astronomy and Geophysics. 7, 1, 31-39, 2018.

490 Ogwala, A., Somoye, E.O., Oyedokun, O., Adeniji-Adele, R.A., Onori, E.O., Ogungbe, A.S.,
 491 Ogabi, C.O., Adejo, O., Oluyo, K.S., Sode, A.T. Analyses of Total Electron Content over Northern
 492 and Southern Nigeria. J. Res. and Review in Sci., 21 – 27, 2018.

493 Onwumechilli, C.A., and Ogbuehi, P.O. *Journal Atmos. Terr. Phys.*, 26, 894, 1964.

494 Rama Rao, P.V.S., Niranjana, K., Rama Rao, B.V., Rama Rao, B.V.P.S., Prasad, D.S.V.V.D. *Proc.*
495 *URSI/ IPS Conference on the ionosphere and Radio wave Propagation*. Sydney, Australia, 1985.

496 Rama Rao, P.V.S., Krishna, S.G., Prasad, J.V., Prasad, S.N.V.S., Prasad, D.S.V.V.D., Niranjana,
497 K. Geomagnetic storm effects on GPS based navigation. *Ann. Geophys.*, 27, 2101 – 2110, 2009.

498 Rama Rao, P.V.S., Krishna, S.G., Niranjana, K., Prasad, D.S.V.V.D. Study of temporal and spatial
499 characteristics of L-band scintillation over the Indian low-latitude region and their possible effects
500 on GPS navigation. *Ann. Geophys.*, 24, 1567 – 1580, 2006a.

501 Rama Rao, P.V.S., Krishna, S.G., Niranjana, K., Prasad, D.S.V.V.D. Temporal and spatial
502 variations in TEC using simultaneous measurements from Indian GPS network of receivers during
503 low solar activity period of 2004 – 2005. *Ann. Geophys.*, 24, 3279 – 3292, 2006b.

504 Rama Rao, P.V.S., Niranjana, K., Prasad, D.S.V.V.D., Krishna, S.G., Uma, G. On the validity of
505 the ionospheric pierce point (IPP) altitude of 350km in the Indian equatorial and low-latitude
506 sector. *Ann. Geophys.*, 24, 2159 – 2168, 2006c.

507 Sethi, N. K., Pandey, V. K., Mahajan, K. K. Comparative study of TEC with IRI model for solar
508 minimum period at low latitude. *Advances in Space Research*, 27, 45 – 48, 2010.

509 Suranya, P.L., Prasad, D.S.V.V.D., Niranjana, K., Rama Rao, P.S.V. Short term variability in foF2
510 and TEC over low latitude stations in the Indian sector. *Indian J. of Radio and Space Phys.*, 44, 14
511 – 27, 2015.

512 Somoye, E.O. Diurnal and seasonal variation of fading rates of E- and F-region echoes during IGY
513 and IQSY at the equatorial station of Ibadan. Indian Journal of Radio and space Physics, 38, 194
514 – 202, 2010.

515 Somoye, E.O., Akala, A.O., Ogwala, A. Day-to-day variability of h'F and foF2 during some solar
516 cycle epochs. Journal Atmos. Solar Terr. Physics, 73, 1915 – 1922, 2011.

517 Stankov, S. M. Trans-ionospheric GPS signal delay gradients observed over mid-latitude Europe.
518 Advances in Space Research, 43, 1314–1324, 2009.

519 Tariku, Y.A. Pattern of GPS-TEC variability over low-latitude regions (African sector) during the
520 deep solar minimum (2008 to 2009) and solar maximum (2012 to 2013) phases. Earth, Planets,
521 and space. 67, 35, 2015.

522 Titheridge, J.E. Changes in atmospheric composition inferred from ionospheric production rates.
523 J. Atmos. Terr. Phys., 36, 1249 – 1257, 1974.

524 Wanninger, L. Effects of the equatorial ionosphere on GPS. GPS World, 2, 48, 1993.

525 Wu, C.C., Liou, K., Shan, S.J., Tseng, C.L. Variation of ionospheric total electron content in
526 Taiwan region of the equatorial anomaly from 1994 – 2003. Adv. Space Res., 41, 611 – 616, 2008.

527

528